

Research Paper**IN SILICO OPTIMIZED MECHLORETHAMINE BASED
DRUG STRUCTURES TARGETING BRAIN
AND SPINAL CORD TUMORS****ABSTRACT**

Aims: Brain and spinal cord tumors are the third most common type of childhood cancer following leukemia and lymphoma. The treatment of brain tumors for children is usually different than for adults. Mechlorethamine (mustine) itself is a bifunctional alkylating cytotoxic vesicant. Eleven variants of mechlorethamine are presented in this study that possess molecular properties enabling substantial access to tumors of the central nervous system.

Methodology: Following extensive in silico search and identification of potential drug structures, the conclusive set of brain penetrating structures were compiled. Extensive characterization of structure properties was accomplished followed by multivariate numerical analysis utilizing pattern recognition and statistical analysis.

Results: All twelve compounds (including mechlorethamine) exhibited zero violations of Rule of 5, indicating favorable bioavailability. The range in Log P, formula weight, and polar surface area for these compounds are: 1.554 to 3.52, 156.06 to 324.12, and 3.238 to 20.240, respectively. The physicochemical properties of all 12 compounds are very highly correlated (by Pearson $r > 0.9900$). High resolution hierarchical cluster analysis determined that agent 2

46
47 and 6 are most similar to the parent compound mechlorethamine. The average
48
49 Log P, formula weight, polar surface area, and molecular volume are 2.446,
50
51 235.433, 8.58, and 213.8 A³, respectively. Nonhierarchical K-means cluster
52
53 analysis indicated that agents 2, 6, and 12 are most similar to mechlorethamine
54
55 and multiple regression analysis of multivariate data set of molecular properties
56
57 produced a model that will enable the design of similar alkylating agents.
58
59 Conclusion: These eleven drug designs possess attributes that effectuate high
60
61 permeation into the central nervous system.

62
63
64 **Key words:** brain tumors, astrocytomas, glioma, mechlorethamine, mustine

65
66 **Abbreviations:** PSA, polar surface area; CNS, central nervous system; MV,
67 molecular volume; NO, number of nitrogen and oxygen atoms; BB, logarithm
68 value of brain to plasma concentration ratio; Log(BB), log value of BB.

69 70 **1. INTRODUCTION**

71
72 Brain and spinal cord tumors are the third most common type of childhood
73
74 cancer, with only leukemia and lymphoma in greater occurrence. The cancers
75
76 occurring in the central nervous system (CNS) can be primary (tumors that
77
78 begin in the CNS) and metastatic (tumors formed from cancer cells beginning
79
80 in other parts of the body). Types of childhood brain and spinal cord tumors
81
82 include: astrocytomas, atypical teratoid tumor, brain stem glioma, CNS
83
84 embryonal tumor, CNS germ cell tumor, craniopharyngioma, ependymoma,
85
86 medulloblastoma, spinal cord tumors, and supratentorial primitive neuro
87
88 ectodermal tumors.

89
90 Mechlorethamine (mustine, mustargen, chlorethazine, chlormethine) is a
91

92 nitrogen mustard agent having antineoplastic and immunosuppressive activity.
93
94 Mechlorethamine alkylates DNA, especially at the 7-Nitrogen site of guanine,
95
96 which induces interstrand crosslinking and inhibition of DNA repair. It is a
97
98 light yellow brownish, hygroscopic, crystalline powder that is very soluble in
99
100 water and alcohol. There are approximately 20,000 new cases of primary
101
102 CNS tumors in the United States every year [1]. Growth of the CNS tumors is
103
104 at the considerable expense of other structure contained within the CNS,
105
106 therefore symptoms depend on the location of tumor [1]. Symptoms include:
107
108 confusion, headache, nausea, vomiting papilledema, seizures, and cognitive
109
110 impairment ^[1].

111
112 Metastases based tumors are the most common type of cancer of the CNS,
113
114 which appear to be on increase [2]. The pathophysiology of brain
115
116 metastases is very important and influences the efficacious of therapies to target
117
118 brain tumor growth [2]. Studies conducted in Korea have shown females to be
119
120 more inclined to CNS tumors (1.43:1) with the most common tumor to be
121
122 meningioma (31.2%) followed by glioblastoma (30.7%) and malignant primary
123
124 tumors (19.3%) [3]. Patients of less than 19 years of age will most commonly
125
126 have germ cell tumors and embryonal/medulloblastoma [3].

127
128 While breast cancer is the most common malignancy within women in the
129
130 United States, the total incidence of brain metastases of breast cancer is
131
132 a significant 30% [4]. The incidence of brain metastases is on the increase
133
134 with breast cancer patients [4]. The development of CNS metastases with breast
135
136 cancer depends on prognostic factors including age and negative hormone
137

138 receptor status [5]. However, patients having breast cancer with intramedullary
139 spinal cord metastases tend to improve better than other case types of cancer
140 [6].
141

142
143
144 Interestingly, nearly half of patients with advanced melanoma develop
145 metastases of the CNS, with up to 20% of these patients incur CNS metastases
146 as the first site of relapse [7]. These incidents of CNS metastases rarely
147 benefit from systemic therapy due to lack of penetration into the CNS by the
148 applied chemotherapeutics [7]. The pursuit of novel drugs to treat
149 melanoma is focused on those agents having useful antitumor activity in
150 addition to the capability of crossing the blood-brain barrier of the CNS [7].
151

152
153
154 Autopsy have shown that up to two thirds of cases of metastatic melanoma do
155 have CNS involvement [8].
156

157
158 Left sided primary colon tumors are predominant in cases of brain metastases
159 associated colorectal cancer (CRC), however these cases arise in only 2.3% of
160 total CRC [9]. Greater survival of CRC is also associated with increased survival
161 of the brain metastases [9]. Patients with primary rectal versus primary colon
162 cancer are more likely to develop bone metastases which has an association
163 to brain metastases as well [10]. Bone metastases among CRC patients is
164 more common with increased numbers of active systematic agents received
165 by the patient [10].
166
167

168
169 These outcomes of clinical studies clearly reveal the need for novel antitumor
170 agents that have effective antineoplastic activity but with molecular properties
171 enabling the penetration of the CNS. Albeit the difficulties of CNS penetration
172
173
174
175
176
177
178
179
180
181
182
183

184 is substantial due to the blood brain barrier, the design of molecular structures
185
186 that can effectuate CNS infiltration are crucial for the treatment of pediatric
187
188 brain tumors.

189 **2. MATERIALS AND METHODS**

190 **2.1 MOLECULAR MODELING**

191
192 Molecular properties and modeling was accomplished by utilizing
193
194 ACD/ChemSketch modeling v. 10.00 (Advanced Chemistry Development,
195
196 110 Yonge Street, Toronto Ontario, M5C 1T4 Canada). Various properties; polar
197
198 surface area, violations of Rule of 5, molecular volume, number of
199
200 oxygens, nitrogens, amines, hydroxyls, etc were determined using Molinspiration
201
202 (Molinspiration Cheminformatics, Nova ulica 61, SK-900 26 Slovensky Grob,
203
204 Slovak Republic). In silico structure search for substituent replacement was
205
206 accomplished using Chemical substructure and similarity search with MolCart
207
208 Chemical Data Base (Molsoft L.L.C. 3366 North Torrey Pines Court, Suite 300,
209
210 La Jolla, CA 92037 U S A).

211 **2.2 PATTERN RECOGNITION**

212
213 To identify underlying associations/patterns within the multivariate data set
214
215 required the use of various pattern recognition techniques. Included in
216
217 the analysis is hierarchical cluster analysis accomplished by KyPlot v. 2.0 Beta
218
219 15 (copyright Koichi Yoshioka 1997-2001). ANOSIM (analysis of similarity),
220
221 95% ellipses, and non-hierarchical K-means cluster analysis were performed by
222
223 PAST v. 2.04 (copyright Oyvind Hammer, D.A.T. Harper 1999-2008).
224
225

226 **2.3 NUMERICAL ANALYSIS**

227
228
229

230 Statistical analysis of all numerical data including correlation analysis by
231
232 Pearson r was performed by Microsoft EXCEL (EXCEL 2003, copyright 1985-
233
234 2003). Multiple regression analysis of molecular properties was accomplished
235
236 by GraphPad InStat v. 3.00 for Windows 95 (GraphPad Software, San Diego
237
238 California USA).

241 **3. RESULTS & DISCUSSION**

242
243 With the appearance of brain metastases occurring in up to 40% of cancer
244
245 patients (with increasing frequency) [11] the investigation of new cytotoxic
246
247 agents is definitely warranted. Lung cancer, breast cancer, and skin melanoma
248
249 are the commonest sources of brain metastases [11]. While whole brain
250
251 radiotherapy (WBRT), with or without surgery, and systemic chemotherapy
252
253 have levels of success, the later neurotoxicity of WBRT treatment is not
254
255 insignificant [11,12]. Several clinical outcomes applying chemotherapy for
256
257 childhood brain tumors are now presented to substantiate the elucidation
258
259 of small molecule antitumor agents to enhance/improve clinical outcome.
260
261 Nitrogen mustard (mechlorethamine), in addition with procarbazine, vincristine,
262
263 and prednisone, when delivered over a 12 year period resulted in halted
264
265 disease progression in 73% of children with medulloblastoma (some with
266
267 complete remission for > 10 years) [13]. This regimen resulted in 50% long
268
269 term survival with children having anaplastic glioma but < 30% response
270
271 with brain stem gliomas [13].

272
273 Mechlorethamine, vincristine, procarbazine, and prednisone (MOPP) for
274
275 treatment of childhood brain tumors has been shown to be well tolerated

276
277 and improves neurodevelopmental outcome [14] and postpones the
278
279 debilitating consequences of radiotherapy [15]. Clinical evidence supportive
280
281 for mechlorethamine (nitrogen mustard) type constructs for targeting tumors
282
283 include the following: promising response in adult high grade glioma [16],
284
285 successful treatment of child Hodgkin disease [17], and effective response for
286
287 mycosis fungoides [18,19,20]. Utilizing mechlorethamine as parent construct for
288
289 design of similar compounds with analogous properties appears advantageous.
290
291 The mechlorethamine sort (see structure 1 Figure 1), is a bifunctional
292
293 alkylating nitrogen mustard agent having a small formula weight (156.06) and
294
295 a single methyl group (-CH₃) covalently bonded to the nitrogen atom. Variation
296
297 of this structure is accomplished by substituent search through in silico structure
298
299 search (for substituent replacement) using chemical substructure and similarity
300
301 mining by MolCart Chemical Data Base. Screening for small formula weight
302
303 moieties and minimizing polar surface area (the surface sum over all polar
304
305 atoms, oxygen and nitrogen, also any attached hydrogen atoms) the population
306
307 of agent 2 to 12 is filtered (see Figure 1). Although restricted to analogy of the
308
309 mechlorethamine molecule, there is considerable diversity in structural
310
311 substituents within 2 to 12. Notably there is aromatic ring (agent 4, 10, and
312
313 11), aliphatic carbon chains (agent 5, 6, 7), amine groups (agent 5, 9), and
314
315 other substructure. Beginning with mechlorethamine but building a diverse
316
317 variety of substituted substituents will be shown to enable a multifariousness
318
319 in pharmaceutical properties. Measured as molecular properties (or descriptors)
320
321 the alteration of druglikeness presents a credible group of designs that will

322
323 permeate the CNS.
324
325 Molecular properties have been utilized to enhance filtering of drug candidates
326
327 by druglikeness and pharmacodynamics to stymie specific physiological
328
329 abnormalities. For evaluation of bioavailability and measurement of CNS
330
331 permeation various molecular properties are shown in Table 1, that include
332
333 Log P (measurement of lipophilic activity), molecular weight, polar surface
334
335 area (PSA), and violations of Rule of 5. Values of Log P have a strong positive
336
337 correlation with molecular weight (Pearson $r = 0.4551$) and molecular volume
338
339 (Pearson $r = 0.5615$). Molecular weight has a very strong positive correlation
340
341 to molecular volume (Pearson $r = 0.9607$) and strong positive correlation to
342
343 number of oxygen and nitrogen atoms (Pearson $r = 0.6365$). Polar surface
344
345 area has a strong positive correlation to molecular volume (Pearson $r = 0.4070$).
346
347 Molecular polar surface area is a property that has been shown to correlate
348
349 well with passive molecular transport through cellular membranes, allowing
350
351 prediction of transport properties of drugs [21]. Examining PSA values for this
352
353 group of structures confers the capacity that 1 through 12 (see Figure 1) will be
354
355 more than 85% absorbed via the intestinal tract following oral administration ^[21].
356
357 Previous investigations have shown that PSA can be effectively utilized to
358
359 discriminate poorly from highly absorbed drugs [22]. In addition, those studies
360
361 concluded that drugs have PSA less than 60 Angstroms² are completely
362
363 absorbed by the intestinal tract [22]. Notably all nitrogen mustard agents 1
364
365 through 12 have PSA attributes well below 60 Anstroms² (the maximum value
366
367 is 22.24 Angstroms² of agent 10).
368

369 The Rule of Five is developed to evaluate druglikeness (a chemical compound
370 with a certain pharmacological or biological activity), and properties that would
371 make it a likely orally active drug in humans [23]. Druglikeness is a qualitative
372 measure of the extent of drug-like action of a substance. Drugs that are
373 administered orally must pass through the intestinal lining and be transported in
374 aqueous blood, followed by penetration of the lipid cellular membrane to reach
375 the inside of a cell for pharmaceutical activity. The Rule of Five states that an
376 orally active drug will have [23]: 1) Not more than 5 hydrogen bond donors (-OH
377 and -NH_n groups); 2) Not more than 10 hydrogen bond acceptors (notably N
378 and O atoms); 3) A molecular weight under 500 g/mol; and 4) A partition
379 coefficient log P less than 5. Structures 1 to 12 have zero violations of Rule
380 of 5, indicating favorable bioavailability for targeting CNS tumors.
381
382
383
384
385
386
387
388
389
390
391
392

393 Cluster analysis is the elucidation of a set of observations into subsets so that
394 objects in the same cluster are most similar within the multivariate data set.
395 Clustering is a method of unsupervised learning, a common method for
396 statistical data analysis. The multivariate data set (Table 1) can be examined to
397 illuminate underlying relations through hierarchical cluster analysis, which will
398 group (cluster) agents 1 to 12 according to highest similarity. The vertical
399 dendrogram of Figure 2 shows that compounds 2 and 6 are most similar to
400 mechlorethamine (agent 1) and are linked at node C. Node D linking agents 3,
401 11, and 9 are determined to be most similar and are connected to 1, 2, and 6 at
402 node A. Compounds 4 and 10 are most similar by properties, joined at node E.
403 Node F links agents 5, 12, 7, and 8 (mutually similar), which are linked with 4 and
404
405
406
407
408
409
410
411
412
413
414

415 10 at node B. Clearly the data set of Table 1 show descriptors of 1 through 12 to
416
417 have similar numerical values, however higher resolution distinguishes 2 and
418
419 6 to be the closest to mechlorethamine. K-means nonhierarchical cluster analysis
420
421 will likewise organize objects into clusters in which members have highest
422
423 similarity, however the number of clusters are predetermined. Outcome of
424
425 K-means determined that mechlorethamine (1) is similar to agent 2, 6 and 12;
426
427 with 3, 5, 9, and 11 clustered; lastly are agents 4, 7, 8, and 10. Proficient
428
429 ordination can resolve which structures would have similarity in clinical
430
431 activity and patient response.

432
433 Extraordinary challenges remain with childhood brain tumors and advances
434
435 need to be pursued in devising therapies having less long-term sequelae.

436
437 Sequelae of brain trauma include headache and dizziness, anxiety, apathy,
438
439 depression, aggression, cognitive impairments (including visual and semantic
440
441 memory, attention, and motor coordination), personality changes, mania,
442
443 and psychosis.

444
445 The degree of blood brain barrier (BBB) penetration is commonly assessed
446
447 as the ratio of the steady-state concentrations of the drug in the blood and brain,
448
449 expressed as $\text{Log}(C_{\text{brain}}/C_{\text{blood}})$, or $\text{Log}(BB)$ (where BB is concentration of drug
450
451 in the brain \div concentration of drug in blood) [24]. The determination of $\text{Log}(BB)$
452
453 and BB has been achieved for drugs 1 to 12 which are presented in Table 2.

454
455 Notably the values of BB are high, all values of BB are greater than one which
456
457 indicates drugs 1 to 12 will likely have greater partitioning within the CNS than
458
459 the blood. The relationship to predict this complex mechanism has been
460

461 shown in previous studies to be systematically predicted by the model [24]:
462
463 $\text{Log (BB)} = -0.0148(\text{PSA}) + 0.152(\text{Clog P}) + 0.139$, where PSA is polar surface
464 area and CLog P is calculated partition coefficient Log P. Drugs that have
465 Log (BB) values greater than 0.3 are shown to readily cross the BBB [24]. Note
466
467 that nine of the 12 agents of Figure 1 have Log (BB) greater than 0.3, they are
468
469 1 (mechlorethamine), 2, 3, 5, 6, 7, 8, 9, and 11. Log (BB) values for the
470
471 remaining agents are also high (agents 4, 10, and 12). These relationships
472
473 are determined to valid for passive diffusion consideration [24].
474
475

476
477 Orally active drugs expected to transport passively by transcellular route
478
479 should not have PSA exceeding 120 Angstroms² [25]. For purposes of crossing
480
481 the BBB into the CNS, then PSA should be less than 60 to 70 Anstroms² [25].
482
483 Notably all drugs 1 to 12 have PSA far less that 60 Angstroms² (range is from
484
485 3.238 Angstroms² to 22.24 Angstroms²), so by this criteria agents 1 to 12 will
486
487 pierce the BBB to target tumors of the CNS, see Table 1.
488

489 The partition coefficient Log P is a property which is a composite of components
490
491 that include polarity, molecular size, polarizability, and hydrogen bonding.
492

493 Previous studies have shown distinctly that small molecules penetrate the
494
495 blood brain barrier [26]. Investigators have determined that optimal penetration
496
497 through the BBB is achievable for molecules having a Log P between 1 to 4 in
498
499 value, a formula weight less than 400, and polar surface area less than 90
500
501 Angstroms² [27]. For drugs 1 to 12, see Table 1, the Log P values range from
502
503 1.554 to 3.52, the formula weights are all below 400, and the polar surface areas
504
505 are far less than 90 Angstroms². Therefore all molecules 1 to 12 are determined
506

507 to have highly efficient access to the central nervous system. Structures 7
508 and 8 have been described previously, which established the identical
509 conclusions concerning their effectiveness in CNS penetration for targeting
510 neoplastic tissue [28]. Structures 7 and 8 are two members of a homologous
511 series (homologous series vary by an extra (-CH₂-) from the previous
512 compound) of nitrogen mustard agents and with each addition of (-CH₂-)
513 comes a variation of molecular properties [28]. The synthesis and other
514 features of this group of nitrogen mustard agents are described previously [28].
515
516
517
518
519
520
521
522

523 Two functions of multiple regression analysis are: 1) explanation of relationship
524 among multiple independent variables, and 2) prediction by utilizing multiple
525 independent variables. By applying the molecular properties presented in
526 Table 1, the multiple regression model appears as follows for prediction of
527 formula weight for additional analogous compounds (FW= formula weight,
528 PSA= polar surface area, MV= molecular volume, NO=number of oxygen and
529 nitrogen atoms):
530
531
532
533
534
535

$$536 \text{FW} = 1.756 - (2.113)(\text{Log P}) - (0.9156)(\text{PSA}) + (1.005)(\text{MV}) + (21.254)(\text{NO})$$

537
538 The R² value of 0.9436 indicates at this model explains 94.36% of the model
539 variance. The formula weight of additional similar structures can be estimated
540 by selection of four physicochemical values. Outcome of in silico search and
541 identification of structures falls within a substantially rigid and tight zone of
542 acceptability as indicated by the 95% ellipses (see Figure 3) of Log P and
543 formula weight (i.e. values of 12 agents fall well within 95% confidence region).
544
545
546
547
548
549
550

551 Analysis of similarities (ANOSIM) provides a way to test statistically whether
552

553 there is a significant difference between two or more groups of sampling units.
554
555 The ANOSIM result for descriptors shown in Table 1 is $R = 1.0$ or a large positive
556
557 R (up to 1) signifying significant dissimilarity among these agents based on their
558
559 physicochemical values [29].

560
561 Any type of brain tumor is inherently serious and life-threatening due to
562
563 an infiltrative proliferation. The threat level is consistent with aspects of
564
565 size, location, type, and extent of development. The investigation of novel
566
567 treatment methods should continue and accompanying presentation of
568
569 new drug designs that present credible advantages in clinical response.

570 571 572 **CONCLUSION**

573
574 In summation, a set of eleven novel drug structures are elucidated by
575
576 in silico optimized substituent search that is founded on the successful
577
578 anticancer nitrogen mustard scaffold of mechlorethamine. Brain metastases
579
580 has been linked to breast cancer, advanced melanoma, and colorectal cancer.
581
582 Various molecular properties that enable the transition from blood to CNS
583
584 have been identified and found to be optimal for the twelve agents reported
585
586 here. The Log P numerical values fall between 1.554 to 3.52 which is a
587
588 range well within the BBB piercing range of 1.0 to 4.00. In addition the values of
589
590 PSA range from 3.238 to 22.24 Angstroms², a range well below the upper
591
592 limit for effective CNS penetration at 90 Angstroms². Importantly all twelve
593
594 agents present zero violations of the Rule of 5, indicating a high level of
595
596 druglikeness and favorable bioavailability. The success rate of in silico search
597
598 and identification of suitable CNS targeting antineoplastic structures was less

599
600 than ten percent. Various attributes recounting the inherit potential of small
601
602 molecules applied as chemotherapeutic agents in the treatment of CNS tumors
603
604 have been presented in this study.
605

606
607 **COMPETING INTERESTS:** There are no competing interests.
608

609
610
611 **LEGENDS TO FIGURES**

612
613 Figure 1: The scaffold of mechlorethamine (1) serves as source construct for
614 substituent optimization producing 11 daughter compounds 2 to 12. The
615 outcome includes a diverse type of substituent types: aromatic, aliphatic,
616 amine, and carbonyl. Resultant molecular properties further substantiate
617 the in silico search method and provide a set of compounds that clearly
618 possess efficaciousness in the clinical treatment of CNS tumors.
619

620 Figure 2: Hierarchical cluster analysis (Euclidean distance and single linkage
621 cluster parameters) of molecular properties (see Table 1) show with high
622 resolution the assimilation by mutual similarity. Albeit the molecular properties
623 (see Table 1) indicate very high numerical correlation, the underlying
624 relationships indicate that agents 2 and 6 are most similar to mechlorethamine.
625 Other aggregation of similarity are: 3, 11, and 9; 4 and 10; 5, 13, 7, and 8.
626 Compounds 1, 2, 6, 3, 11, and 9 are joined at node A. Agents 4 and 10 are
627 joined at node E and joined to 5, 12, 7, and 8 at node B.
628

629 Figure 3: Two-way plot of Log P and molecular weight indicates complete
630 inclusion into 95% ellipses. Thus indicating relationship of lipophilicity to
631 molecular weight is inclusive within 95% confidence.
632

633
634
635 **REFERENCES**

636
637 [1] Alomar, SA. Clinical manifestation of central nervous system tumor. Semin
638 Diagn Patho. 2010;27(2):97-104.
639

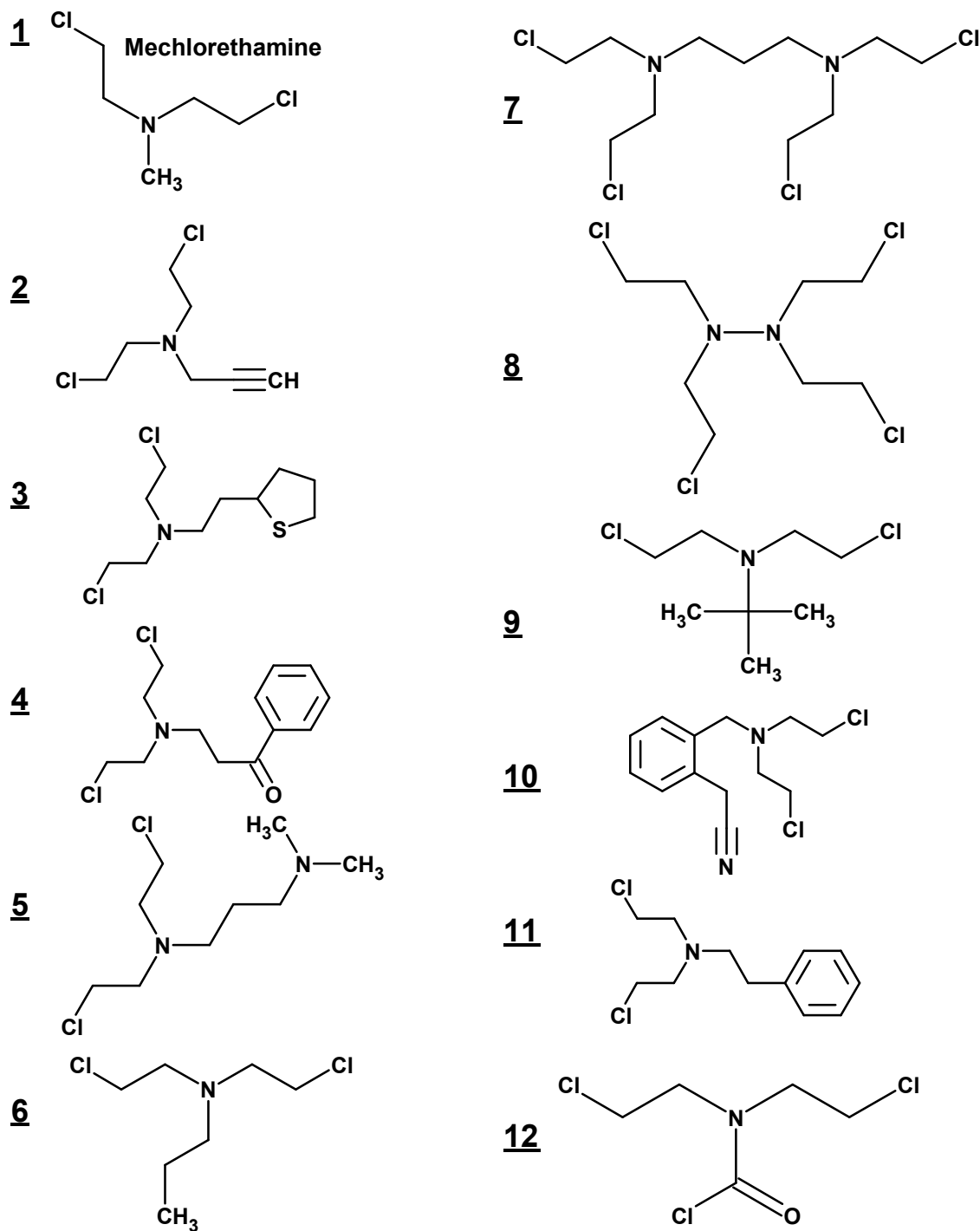
640 [2] Gavrilovic, IT, Posner, JB. Brain metastases: epidemiology and
641 pathophysiology. J Neurooncol. 2005;75(1):5-14.
642

- 643 [3] Lee CH, Jung KW, Yoo H, Park S, Lee SH. Epidemiology of primary brain and
644 central nervous system tumors in Korea. *J Korean Neurosurg Soc.* 2010;48(2):
645 145-152.
646
- 647 [4] Cheng X, Hung MC. Breast cancer brain metastases. *Cancer Metastasis*
648 *Rev.* 2007;26(2-4):635-643.
649
- 650 [5] Kaal EC, Vecht CJ. CNS complications of breast cancer: current and
651 emerging treatment options. *CNS Drugs.* 2007; 21(7):559-579.
652
- 653 [6] Choi HC, Yoon do H, Kim SC, Cho KH, Kim SH. Two separate episodes of
654 intramedullary spinal cord metastasis in a single patient with breast cancer. *J*
655 *Korean Neurosurg Soc.* 2010;48(2):162-165.
656
- 657 [7] Douglas JG, Margolin K. The treatment of brain metastases from malignant
658 melanoma. *Semin Oncol.* 2002;29(5):518-524.
659
- 660 [8] Bafaloukos, D, Gogas H. The treatment of brain metastases in melanoma
661 patients. *Cancer Treat Rev.* 2004;30(6):515-520.
662
- 663 [9] Morgan JP, Fadul CE, Cole BF, Zaki B, Suriawinata AA, Ripple GH, Tosteson
664 TD, Pipas JM. Brain metastases from colorectal cancer: risk factors, incidence,
665 and the possible role of chemokines. *Clin Colorectal Cancer.* 2009;8(2):100-105.
666
- 667 [10] Sundermeyer ML, Meropol NJ, Rogatko A, Wang H, Cohen SJ. Changing
668 patterns of bone and brain metastases in patients with colorectal cancer. *Clin*
669 *Colorectal Cancer.* 2005;5(2):108-113. .
670
- 671 [11] Soffietti R, Ruda,R, Mutani R. Management of brain metastases. *J Neurol.*
672 2002;249(10):1357-1369.
673
- 674 [12] Tsao MN, Lloyd N, Wong R, Chow E, Rakotitch E, Laperriere N. Whole
675 brain radiotherapy for the treatment of multiple brain metastases. *Cochrane*
676 *Database Syst. Rev.* 2006;3(CDO003869):1-10.
677
678
679
- 680 [13] van Eys J, Baram TZ, Cangir A, Bruner JM, Martinez-Prieto J. Salvage
681 chemotherapy for recurrent primary brain tumors in children. *J Pediatr.*
682 1988;113(3):601-606.
683
- 684 [14] Ater JL, van Eys J, Woo SY, Moore B, Copeland DR, Bruner J. MOPP
685 chemotherapy without irradiation as primary postsurgical therapy for brain tumors
686 in infants and young children. *J Neurooncol.* 1997;32(3): 243-252.
687

- 688 [15] van Eys J, Cangir A, Coody D, Smith B. MOPP regimen as primary
689 chemotherapy for brain tumors in infants. *J Neurooncol.* 1985;3(3):237-243.
690
- 691 [16] Coyle T, Baptista J, Winfield J, Clark K, Poiesz B, Kirshner J, Scalzo A,
692 Newman-Palmer N, King R, Graziano S. Mechlorethamine, vincristine, and
693 procarbazine chemotherapy for recurrent high-grade glioma in adults: a phase II
694 study. *J Clin Oncol.* 1990;8(12):2014-2018.
695
- 696 [17] Keskin EY, Gursel T, Uluoglu O, Albayrak M, Kaya Z, Coskun U, Kocak U.
697 Parathyroid adenoma and chondrosarcoma after treatment of pediatric Hodgkin
698 disease. *J Pediatr Hematol Oncol.* 2010;32(7):e294-e296.
699
- 700 [18] de Quatrebarbes J, Esteve E, Bagot M, Bernard P, Beylot-Barry M,
701 Delaunay M, D'Incan M, Souteyrand P, Vaillant L, Corde N, Courville P, Joly P.
702 Treatment of early-stage mycosis fungoides with twice-weekly applications of
703 mechlorethamine and topical corticosteroids: a prospective study. *Arch*
704 *Dermatol.* 2005;141(9):1117-11120.
705
- 706 [19] Galper SL, Smith BD, Wilson LD. Diagnosis and management of mycosis
707 fungoides. *Oncology.* 2010;24(6):491-501.
708
- 709 [20] Kim YH, Martinez G, Varghese A, Hoppe RT. Topical nitrogen mustard in
710 the management of mycosis fungoides: update of the Stanford experience. *Arch*
711 *Dermatol.* 2003;139(2):165-173.
712
- 713 [21] Ertl P, Rohde B, Selzer P. Fast calculation of macular polar surface area as
714 a sum of fragment-based contributions and its application to the prediction of
715 drug transport properties. *J Med Chem.* 2000;43:3714-3727.
716
- 717 [22] Palm K, Stenberg P, Luthman K, Artursson P. Polar molecular surface
718 properties predict the intestinal absorption of drugs in humans. *Pharmaceutical*
719 *Research.* 1997;14(5):568-571.
720
- 721 [23] Lipinski CA, Lombardo F, Dominy BW, Feeney PJ. Experimental and
722 computational approaches to estimate solubility and permeability in drug
723 discovery and development settings. *Adv Drug Del Rev.* 2001;46:3-26.
724
- 725 [24] Clark DE. Rapid calculation of polar molecular surface area and its
726 application to the prediction of transport phenomena. 2. prediction of blood-brain
727 barrier penetration. *J Pharmaceutical Sciences.* 1999; 88(8):815-821.
728
- 729 [25] Kelder J, Grootenhuis P, Bayada D, Delbressine L, Ploemen JP. Polar
730 molecular surface as a dominating determinant for oral absorption and brain
731 penetration of drugs. *Pharmaceutical Res.* 1999;16(10):1514-1519.
732

- 733 [26] van de Waaterbeemd H, Kansy W. Hydrogen bonding capacity and brain
734 penetration. *Chimia*. 1992; 46:299-303.
735
- 736 [27] van de Waterbeemd H, Camenisch G, Folkers G, Chretien JR, Raevsky
737 OR. Estimation of blood-brain crossing of drugs using molecular size and shape,
738 and H-bonding descriptors. *J Drug Targeting*. 1998;6:151-165.
739
- 740 [28] Bartzatt R, Donigan L. Applying pattern recognition methods to analyze the
741 molecular properties of a homologous series of nitrogen mustard agents. *AAPS*
742 *PharmSciTech*. 2006;7(2):E1-E7.
743
- 744 [29] Clarke KR. Non-parametric multivariate analysis of changes in community
745 structure. *Australian Journal of Ecology*. 1993 :18:117-143.

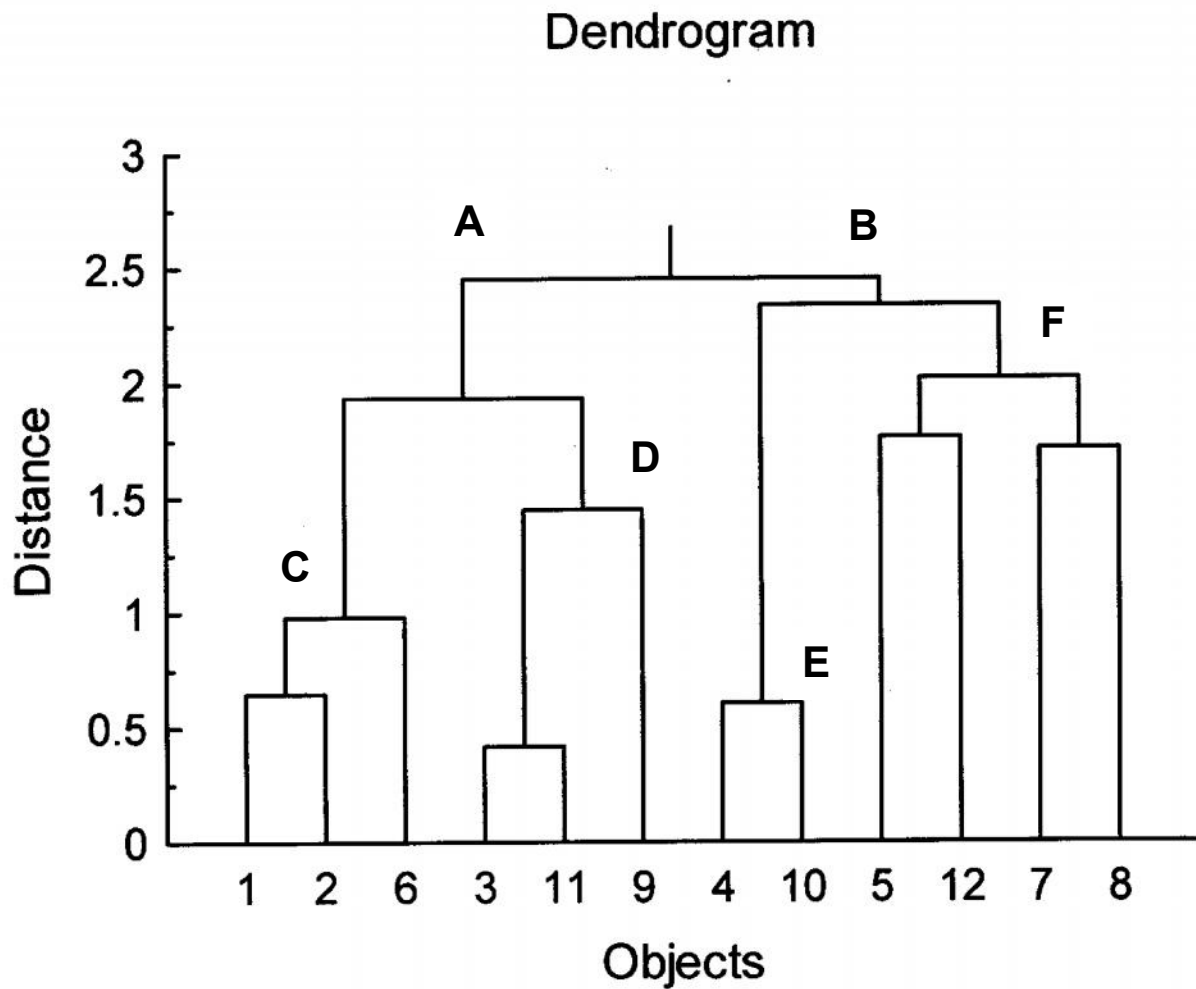
FIGURE 1
Molecular Structures of Anticancer Drugs



746
 747
 748
 749

750
751
752
753

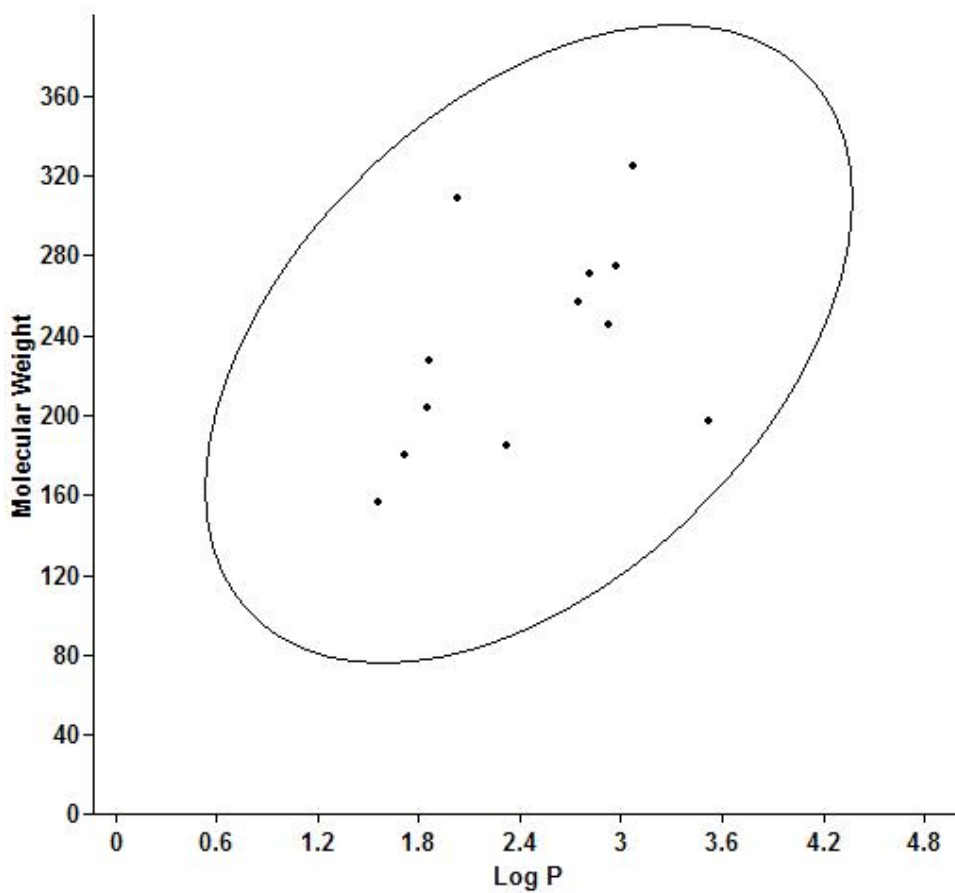
FIGURE 2



754
755
756
757
758
759
760
761
762
763
764

765
766
767
768

FIGURE 3



769
770
771
772
773
774
775
776
777
778
779
780
781

782

783 **Table 1. Molecular Properties**

			Polar Surface Area	Molecular Volume	Nitrogen & Oxygen Atoms	Violations Rule of Five
<u>Drug</u>	<u>Log P</u>	<u>Weight</u>	<u>(Angstroms²)</u>	<u>(Angstroms³)</u>	<u>Oxygen Atoms</u>	<u>Five</u>
1, Mechlorethamine	1.554	156.06	3.238	140.05	1	0
2	1.713	180.078	3.238	158.758	1	0
3	2.739	256.242	3.238	227.821	1	0
4	2.972	274.191	20.309	243.693	2	0
5	1.854	227.18	6.476	216.01	2	0
6	2.32	184.11	3.238	169.86	1	0
7	3.07	324.12	6.476	277.166	2	0
8	2.03	308.04	9.5	274.26	2	0
9	3.52	197.07	5.14	200.53	1	0
10	2.81	270.07	22.24	266.03	2	0
11	2.92	245.07	4.73	230.4	1	0
12	1.85	202.97	15.14	161.33	2	0

784

785

786

787

788

789 **TABLE 2 Numerical Values of Log(BB) and BB**

		BB
<u>Drug</u>	<u>Log (BB)</u>	<u>Cbrain/Cblood</u>
1, Mechlorethamine	0.327	2.12
2	0.351	2.24
3	0.507	3.21
4	0.290	1.95
5	0.325	2.11
6	0.444	2.78
7	0.509	3.23
8	0.307	2.03
9	0.598	3.96
10	0.237	1.73
11	0.513	3.26
12	0.196	1.57

790